The Role of the C-Terminus for Functional Heteromerization of the Plant Channel KDC1

Alessia Naso,[†] Ingo Dreyer,[‡*] Laura Pedemonte,[†] Ilaria Testa,[§] Judith Lucia Gomez-Porras,[¶] Cesare Usai,[†] Bernd Mueller-Rueber,[¶] Alberto Diaspro,[§] Franco Gambale,[†] and Cristiana Picco[†*]

[†]Istituto di Biofisica, Consiglio Nazionale delle Ricerche, 16149 Genoa, Italy; [‡]Universität Potsdam, Institut für Biochemie und Biologie, Abteilung Molekularbiologie, Heisenberg-Gruppe BPMPB, 14476 Potsdam/Golm, Germany; [§]LAMBS-MicroScoBio and IFOM Research Center, Department of Physics, University of Genoa, 16146 Genoa, Italy; and [¶]Universität Potsdam, Institut für Biochemie und Biologie, Abteilung Molekularbiologie, 14476 Potsdam/Golm, Germany

ABSTRACT Voltage-gated potassium channels are formed by the assembly of four identical (homotetramer) or different (heterotetramer) subunits. Tetramerization of plant potassium channels involves the C-terminus of the protein. We investigated the role of the C-terminus of KDC1, a *Shaker*-like inward-rectifying K$^+$ channel that does not form functional homomeric channels, but participates in the formation of heteromeric complexes with other potassium α-subunits when expressed in *Xenopus* oocytes. The interaction of KDC1 with KAT1 was investigated using the yeast two-hybrid system, fluorescence and electrophysiological studies. We found that the KDC1-EGFP fusion protein is not targeted to the plasma membrane of *Xenopus* oocytes unless it is coexpressed with KAT1. Deletion mutants revealed that the KDC1 C-terminus is involved in heteromerization. Two domains of the C-terminus, the region downstream the putative cyclic nucleotide binding domain and the distal part of the C-terminus called K_{HA} domain, contributed to a different extent to channel assembly. Whereas the first interacting region of the C-terminus was necessary for channel heteromerization, the removal of the distal K_{HA} domain decreased but did not abolish the formation of heteromeric complexes. Similar results were obtained when coexpressing KDC1 with the KAT1-homolog KDC2 from carrots, thus indicating the physiological significance of the KAT1/KDC1 characterization. Electrophysiological experiments showed furthermore that the heteromerization capacity of KDC1 was negatively influenced by the presence of the enhanced green fluorescence protein fusion.

INTRODUCTION

K$^+$ is involved in several key cellular functions in plants such as the maintenance of membrane potential, enzyme activation, stomatal movements, and tropisms (1,2,3). Over the past decade, reverse genetics and electrophysiological studies have revealed the presence of several families of K$^+$ channels. Voltage-gated potassium channels have been found in a variety of plants. They are tetramers composed of four α-subunits. Each subunit is a transmembrane protein built of six transmembrane domains (called S1–S6) and a pore-forming linker domain (P) between S5 and S6. Because of their structural similarity to the *Shaker* K$^+$-channel from *Drosophila melanogaster*, voltage-gated ion channels from plants are also widely termed plant *Shaker*-like K$^+$ channels. In plants, these channels are involved in the uptake of K$^+$ from the soil and its redistribution throughout the plant (2).

Despite their common structure, members of the family of plant *Shaker*-like K$^+$ channels exhibit an astonishing diversity at the functional level. They can be classified into at least three different subfamilies, including inward-rectifying channels (K_{in} channels) that open upon hyperpolarization and enable the uptake of potassium ions, outward-rectifying channels (K_{out} channels) that open upon depolarization and enable the release of K$^+$. The third subfamily of weak-rectifying channels (K_{weak} channels) comprises channels that are uniquely regulated by phosphorylation. Depending on their phosphorylation status, they gate either similar to K_{in} channels or behave as K$^+$-selective leaks (4–7).

The tetrameric structure of potassium channels suggested the formation of homo- and heteromeric plant potassium channels. Indeed, heteromeric plant K$^+$ channels were observed i), between different members of the K_{in} subfamily (8–10), ii), between different members of the K_{out} channel subfamily (11), and iii), between members of the K_{weak} and the K_{in} subfamilies (12–14). Over and above, heteromeric channels were observed when K_{in} channel α-subunits were coexpressed with a certain type of α-subunits that could not be characterized as functional homomers when expressed alone (8,15–21). It is therefore speculated that α-subunits of this type form a fourth subfamily of silent channels (K_{silent}) that have only a modulatory effect on other K$^+$ channels. The model systems for members of this class are AtKC1 from *Arabidopsis thaliana* (8,16,21) and KDC1 from the carrot *Daucus carota* (15,17–20,22).

To date, however, it is not clear why K_{silent} channels are not functional when expressed alone in *Xenopus* oocytes. After studies by Bregante et al. (20) and Duby et al. (21), their roles in plant cells are more clear now, but expression mechanisms in *Xenopus* still deserve further investigation. Specifically it is not clear which parts of the channel are

---

important for the heteromerization and evolvement of the modulatory effect on K_{in} channels. In this study we used the well-characterized K_{in}-K_{silent} pair KAT1-KDC1 (15,18, 19) to address this question. We tagged the channel α-subunits with the reporter protein GFP to analyze the expression of the channels and used the yeast two-hybrid system to identify domains that are important for the physical interaction of the C-termini of the proteins. Moreover we performed electrophysiological experiments to functionally characterize the heteromeric assembly of the channels. To evaluate in as much our results on this model pair can be generalized to KAT1-like channels in carrots, we tested the coexpression of KDC1 with KDC2, a KAT1 homolog from *Daucus carota*, which shares an overall identity of 63% with KAT1 (23).

MATERIALS AND METHODS

Recombinant DNA techniques

Standard methods of plasmid DNA preparation, polymerase chain reaction, restriction enzyme analysis, agarose gel electrophoresis, and bacterial transformation were applied (24). Chimeras and deletions were created by polymerase chain reaction-based techniques.

Expression in *Xenopus* oocytes

Oocytes were isolated from *Xenopus laevis* females and injected or coinjected (at 1:1 weight ratio, unless otherwise specified) with cRNA (0.4 $\mu g/\mu l$) encoding for the tested constructs using a Drummond "Nanoject" microinjector (50 nl/oocyte). Whenever a comparison was made, experiments were performed on the same batch of oocytes, from the same frog, and always on the same day from the injection.

Confocal microscopy

The region encoding for the enhanced green fluorescence protein (EGFP) was fused in frame to the 3′ end of the regions coding for the channel subunits of interest, by using recombinant DNA techniques. Fusion proteins were expressed in *Xenopus* oocytes. To distinguish the plasma membrane fluorescence induced by EGFP-tagged membrane proteins, oocytes were also injected by the fluorescent cytosolic calcium marker Fura Red. EGFP (Em: 509 nm) and Fura Red (Em: 665–685 nm) fluorescences were analyzed by a Nikon Eclipse C1 confocal laser scanning microscope equipped with a 60× PlanApo oil-immersion objective. Both EGFP and Fura Red were excited at 488 nm, and emissions were monitored with suitable filters. Z-stacks of 80 images were built up starting from the plasma membrane within the oocyte (0.5 μM steps). EGFP and Fura Red fluorescences were discriminated using the spectral unmixing technique (25–27). All measurements were averaged (mean ± combined standard error) from >20 independent scans in several oocytes ($N \geq 8$) from more than four donor frogs. Combined standard error takes into account the statistical standard error and the uncertainty related to the confocal microscope resolving power, according to the expression $SE+IR/(12)^{1/2}$, where IR is the instrument resolution (28). Experiments were done at room temperature with oocytes bathed in Barth's solution.

Electrophysiology

Whole-cell K^+ currents were measured with a two-microelectrode home-made voltage-clamp amplifier (designed by F. Conti), using 0.2–0.4 MΩ electrodes filled with 3 M KCl. The following standard bath solution was used (in mM): 100 KCl, 2 $MgCl_2$, 1 $CaCl_2$. 1 $LaCl_3$, 10 MES/Tris, pH 5.6. 1 mM $LaCl_3$ was added to the bath solution to inhibit oocyte endogenous currents elicited by potentials more negative than −160 mV. It was verified in advance that in our working conditions La^{3+} had no effect on the K^+ channels under investigation. Zn^{2+} was added to the external standard solution to a final concentration of 1 mM as $ZnCl_2$.

The relative open probability was obtained dividing the steady-state currents by (V-V_{rev}) and normalized to the saturation value of the calculated Boltzmann distribution. Unless otherwise indicated, experimental data points represent mean values of at least seven experiments ± SE. Half-activation potentials ($V_{1/2}$) and apparent gating charge, z, were determined by fitting experimental points with a single Boltzmann isotherm of the form: $P_{open}= 1/[1+\exp(zF(V-V_{1/2})/RT)]$. Activation time constants τ_1, τ_2 were obtained by fitting the activation curves with the sum of two exponentials. For clarity reasons only the slower, most reliable component, τ_2 is plotted (see Fig. 7 *B*).

Yeast two-hybrid interaction tests

The two-hybrid technique was used to identify cytoplasmic domains responsible for the heteromerization of KDC1 and KAT1. Constructs specified in the figures were cloned into the pLexPD vector (29) in fusion with the LexA DNA-binding domain, and into the pAD-GAL4 vector (Stratagene, Amsterdam, The Netherlands) in fusion with the GAL4 activator domain. Combinations of these constructs were used to cotransform the L40 yeast strain, which has two independent reporter genes, *lacZ* and *HIS3*, under the control of two different promoters. The promoter of *HIS3* comprises the *HIS3* TATA box fused to four copies of the LexA operator and the promoter of *LacZ* comprises the GAL1 TATA box fused to eight copies of the LexA operator. Because of the different promoter structures the expression of Imidazoleglycerol-phosphate dehydratase (*HIS3*) and β-galactosidase (*LacZ*) can differ and usually depends on the protein fused to the LexA DNA-binding domain. Therefore, double transformants were tested in drop tests for both, growth in the absence of histidine in the medium and for β-galactosidase activity. Yeast colonies were picked and resuspended in 100 μl of H_2O. These suspensions (10 μl) were dropped on solid Leu⁻Trp⁻His⁻ medium containing 5-bromo-4-chloro-3-indolyl-beta-D-galactopyranoside. Plates were incubated for 5 days at 30°C.

RESULTS

Fluorescence points out that, when expressed, KDC1 alone is not targeted to the oocyte membrane

The K^+ channel α-subunit KDC1 modified the transmembrane current characteristics of the potassium channel KAT1 when both proteins were coexpressed in *Xenopus* oocytes. However, when only KDC1 was expressed, we did not observe any current in the experimentally accessible voltage-range from −250 mV to +100 mV (15,18,19). This lack of functionality may be alternatively explained in different ways: a), homomeric KDC1 channels are expressed and targeted to the plasma membrane but are closed in the entire voltage-range from −250 mV up to +100 mV, b), homomeric KDC1 channels are expressed but not targeted on the plasma membrane, c), homomeric KDC1 channels are not expressed at all. To discriminate between these possibilities, we tagged KAT1 as well as KDC1 with EGFP and expressed these fusion proteins alone or in combination with untagged K^+ channel α-subunits in oocytes. The EGFP fluorescence from the labeled KAT1 protein was clearly detected

in a layer ~5 μM thick, that probably represents the oocyte membrane and its invaginations (Fig. 1, *A–C* and *G*) (30). In electrophysiological experiments performed on the same oocytes, typical KAT1 currents were observed (data not shown), thus confirming that the fusion protein KAT1-EGFP was targeted to the plasma membrane (see also (31)). Similarly, when KDC1-EGFP was coexpressed with the unlabeled KAT1, the EGFP fluorescence was observed at the superficial layer of the oocyte (Fig. 1, *E* and *G*). This signal could only originate from KDC1-EGFP because when only the unlabeled KAT1 was expressed, only a faint autofluorescence with spectral features different from the EGFP spectrum was observed (Fig. 1, *F* and *G*). In contrast, only a minor

number (5/21) of oocytes, injected with the fusion protein KDC1-EGFP, displayed an EGFP emission (Fig. 1, *D* and *G*).

To discriminate whether this fluorescence can be ascribed to proteins present in the plasma membrane or confined in the cytosol, the fluorescent cytosolic calcium marker Fura Red, was microinjected in oocytes. The normalized EGFP and Fura Red fluorescence intensity distributions were then analyzed along an oocyte radius. Well-defined differences were observed between the constructs; the fluorescence peaks from the fusion protein KAT1-EGFP and from the coexpressed KAT1/KDC1-EGFP were localized externally to the Fura Red fluorescence peak (Fig. 2, *A*, and *B*, *left panel*). On the contrary, when only KDC1-EGFP was
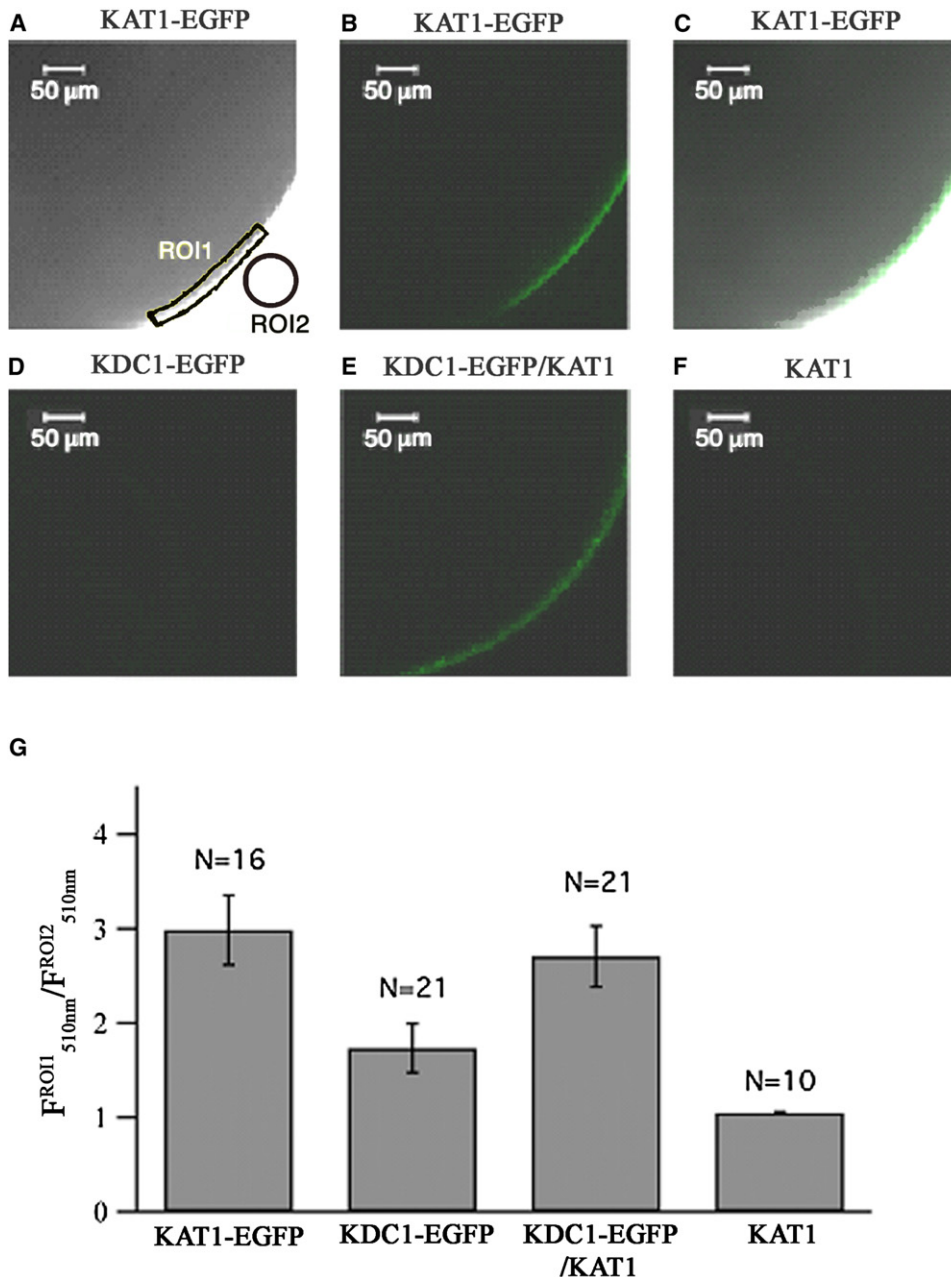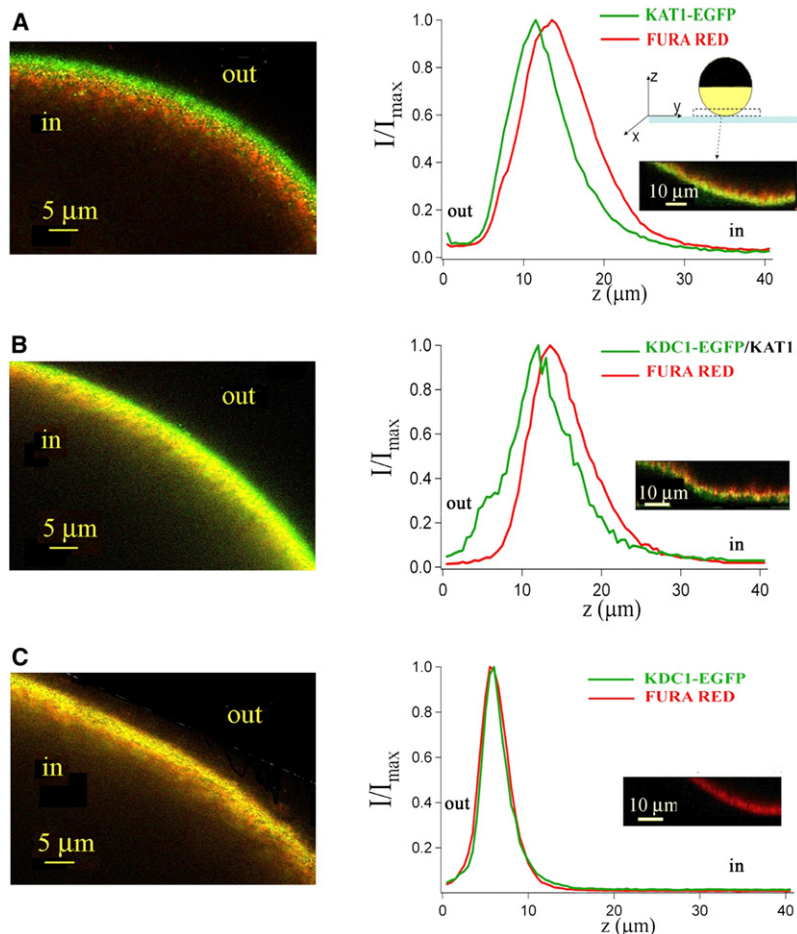

FIGURE 1 KDC1 is efficiently targeted to the membrane only when coinjected with KAT1. Confocal laser-scanning microscopical analyses on oocytes expressing KAT1-EGFP (*A–C*), KDC1-EGFP (*D*), KAT1/KDC1-EGFP (*E*), and KAT1 (*F*). Panel *A* shows the transmission light signal, panels *B*, *D–F* show the fluorescence signal, and panel *C* shows the superimposition of transmission and fluorescence signal. (*G*) Relative fluorescence at 510 nm measured at the external layer of the oocyte (region of interest 1, ROI1, yellow marked area in *A*) and outside the oocyte (ROI2, orange marked area in *A*, taken as the reference value). Data are shown as mean $\pm$ SE (N = number of experiments).

FIGURE 2 KDC1 is targeted to the membrane only in tandem with KAT1. Confocal laser-scanning microscopical analyses on oocytes expressing KAT1-EGFP (*A*), KAT1/KDC1-EGFP (*B*), and KDC1-EGFP (*C*) microinjected with Fura Red. The left column shows the fluorescence collected from an *x-y* plane of the oocyte. Panels *A* and *B* show a green layer (belonging to GFP signal) external to the red one (belonging to Fura Red signal); the yellow layer is due to the colocalization of the two fluorophores. In panel *C* there is no green layer. The right column shows the results obtained by a spectral unmixing analysis, applied on every injected oocyte: traces show normalized fluorescence intensity for a particular region of interest (ROI) of the two fluorophores as a function of the distance *z* (0 coincides with the slide plane and 40 μm with the most internal plane of the oocyte reached). The distance between the two peaks, d(EGFP-Fura Red), is significant in the case of KAT1-EGFP (2.6 $\pm$ 0.3 μm) and KAT1/KDC1-EGFP (2.5 $\pm$ 0.3 μm), whereas for KDC1-EGFP the two peaks practically coincide ($-0.5 \pm$ 0.3 μm). Data are mean values $\pm$ SE from more than 20 ROI.

injected, the green and red fluorescence distributions were fully overlapped, suggesting that KDC1-EGFP was located in the cytosol (Fig. 2 *C*, *left panel*). Fig. 2 (*right panel*) displays the normalized intensity distributions of both EGFP and Fura Red fluorescences for the different constructs in the left panel. The average distance between the EGFP (*green trace*) and the Fura Red (*red trace*) fluorescence maxima is 2.6 $\pm$ 0.3 μm for KAT1-EGFP, 2.5 $\pm$ 0.3 μm for KAT1/KDC1-EGFP, and approximately zero ($-0.5 \pm$ 0.3 μm) for KDC1-EGFP (N $\geq$ 20).

These results suggest that KDC1 alone, when expressed, is not targeted to the plasma membrane, whereas the coexpression of KDC1 and KAT1 targets the complex to the oocyte membrane.

The C-termini of KAT1 and KDC1 interact, whereas the N-termini do not

To verify the role of different protein segments to heteromeric KAT1/KDC1 assembly, we performed experiments by using various methodological approaches on different truncated forms of the C-terminus of KDC1 and KAT1. In this part of the study, we employed the yeast two-hybrid system to identify regions that are involved in the channel heteromerization.

In a first approach, we fused the cytosolic N-terminus of KAT1 (=KAT1-M1_M64) and of KDC1 (=KDC1-M1_A64) to the LexA DNA binding domain and to the GAL4 activator domain, respectively. The fusion proteins were pairwise coexpressed in the yeast strain L40, which comprises the two reporter genes *HIS3* and *LacZ*. When the cotransformants were tested on histidine-free media no growth could be observed. Likewise, no β-galactosidase activity was monitored. On media containing 5-bromo-4-chloro-3-indolyl-beta-D-galactopyranoside no blue dye formation was detected (data not shown).

In a second approach, we included the cytosolic C-termini of KDC1 (Ct-KDC1=KDC1-A310_F629) and KAT1 (Ct-KAT1=KAT1-T308_N677) in our tests (Fig. 3 *A*, *i*, *ii*). No indications for physical protein-protein interactions between N- and C-termini were observed (data not shown). In contrast, clear reporter gene expressions were observed when the KAT1 C-terminus was fused to the LexA DNA binding domain and the KDC1 C-terminus to the GAL4 activator domain (Fig. 3 *A*). Similarly, when assessing the inverse fusions we observed only for the KAT1/KDC1 pair the expression of the *LacZ* reporter gene. On the contrary, the histidine reporter gene was active in all combinations with the KDC1 C-terminus, LexA fusion indicating an autoactivity
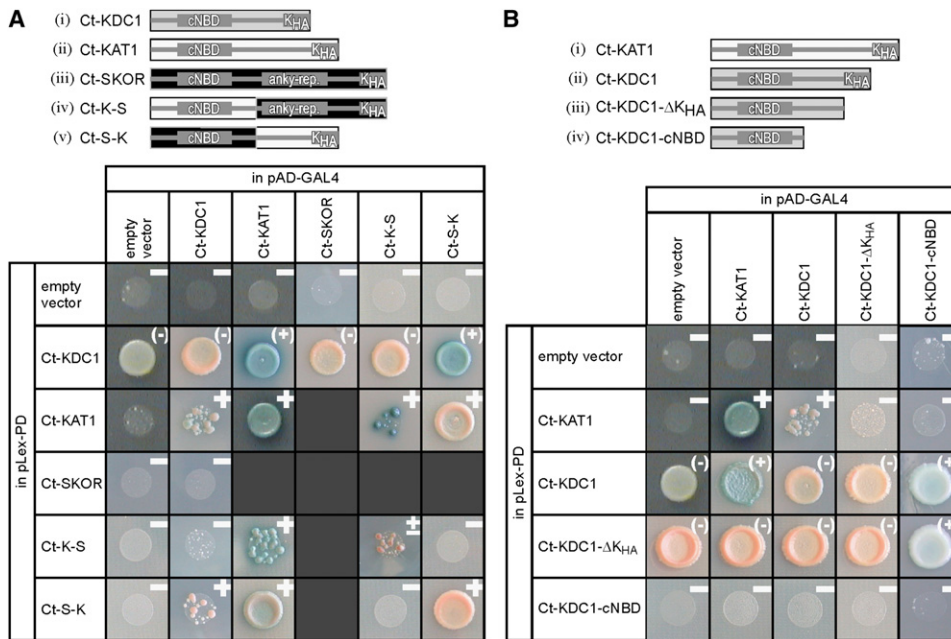
FIGURE 3 Yeast two-hybrid studies on the interaction between the C-termini of potassium channels. Interactions were monitored in a drop test on Leu⁻-Trp⁻-His⁻ medium containing 5-bromo-4-chloro-3-indolyl-beta-D-galactopyranoside. Blue dye formation and, in part, growth report the physical association of the coexpressed fusion proteins. A positive answer is denoted by a ''+'', a negative answer by a ''−''. The presented results are representatives of at least three independent experiments each. Note that the fusions of Ct-KDC1 and Ct-KDC1-ΔK_{HA} to the LexA binding domain enable yeast to grow on histidine-free medium even in the absence of an interacting protein (Ct-KDC1 + empty vector, Ct-KDC1-ΔK_{HA} + empty vector). In these cases, *HIS3* is not a suitable reporter gene for protein-protein interactions, and therefore only the blue dye formation was interpreted as a positive answer (indicated as (+)). (*A*) Identification of intermolecular interactions between the C-termini of KAT1, SKOR, and KDC1. A schematic illustration of the tested C-termini and chimeras is shown in the upper panel. Parts originating from KDC1 are illustrated by gray rectangles, parts from KAT1 by white rectangles, and parts from SKOR are shown as black rectangles. The C-terminal regions Ct-KDC1 (=KDC1-A310_F629) (*i*), Ct-SKOR (=SKOR-D338_T828) (*ii*), Ct-KAT1 (=KAT1-T308_N677) (*iii*), Ct-K-S (=KAT1-T308_D544-SKOR-P574_T828) (*iv*), Ct-S-K (=SKOR-D338_D573-KAT1-T545_N677) (*v*) were fused to the LexA DNA binding domain of the vector pLexPD and to the GAL4 activator domain of the vector pAD-GAL4. The interactions between Ct-SKOR and Ct-KAT1, Ct-K-S, and Ct-S-K were tested and reported earlier (11). (*B*) Identification of structural domains of KDC1 being responsible for the interaction with KAT1. A schematic illustration of the tested full-length and truncated C-termini is shown in the upper panel. Parts originating from KDC1 are illustrated by gray rectangles, parts from KAT1 by white rectangles: the C-terminal regions Ct-KAT1 (=KAT1-T308_N677) (*i*), Ct-KDC1 (=KDC1-A310_F629) (*ii*), Ct-KDC1-ΔK_{HA} (=KDC1-A310_T578) (*iii*), and Ct-KDC1-cNBD (=KDC1-A310_F495) (*iv*) were fused to the LexA DNA binding domain of the vector pLexPD and to the GAL4 activator domain of the vector pAD-GAL4.

of this construct, which sets limits for the interpretation of these data. Nevertheless, the combined results indicate that the C-termini of KAT1 and KDC1 physically interact.

The K_{HA} domain of the KAT1 C-terminus is responsible for the interaction with KDC1 in yeast

Next we tested the interaction of the KDC1 C-terminus with the C-terminus of the plant K_{out} channel SKOR (Ct-SKOR= SKOR-D338_T828). There were no indications for a physical interaction between the KDC1 and SKOR C-termini (Fig. 3 *A*). Based on this result we narrowed down in KAT1 the region that is responsible for the interaction with KDC1. We created two chimeras between the C-termini of KAT1 and SKOR, Ct-K-S, and Ct-S-K, as indicated in Fig. 3 *A* (*iv*, *v*). When we tested these constructs in the yeast two-hybrid system against Ct-KDC1, reliable reporter gene expressions were only monitored with Ct-S-K. This result suggests that the distal part of the KAT1 C-terminus is responsible for the interaction with KDC1. In contrast, the KAT1 C-terminus appears to interact with both chimeras, Ct-K-S and Ct-S-K, but preferentially with the chimera Ct-K-S comprising the first part of the KAT1 and the second part of the SKOR C-terminus (Fig. 3 *A*).

The K_{HA} domain of KDC1 is responsible for the interaction with the KAT1 C-terminus in yeast

Finally, we investigated which part of the KDC1 C-terminus was responsible for the interaction with the KAT1 C-terminus. For this purpose, we deleted from the KDC1 C-terminus the K_{HA}-domain (last 51 amino acids; Ct-KDC1-ΔK_{HA}; Fig. 3 *B*, *iii*) and a larger stretch of 134 amino acids right after the cyclic nucleotide binding domain (Ct-KDC1-cNBD; Fig. 3 *B*, *iv*). Both domains have their equivalents in all other voltage-gated plant K⁺ channels. Nevertheless, their roles are controversially discussed. It is widely accepted, for instance, that the presence of the cNBD is essential for channel formation (11,32,33). The specificity for channel assembly, however, is not determined by this domain (11). A different role was assigned to the K_{HA} domain, a region at the carboxy-terminal end of plant *Shaker*-like K⁺ channels, which comprises two high-homology blocks enriched for hydrophobic and acidic amino-acid residues, respectively. This domain is somehow involved in the interaction between channel α-subunits, but its presence is not essential for functional channel formation (32,34).

When both deletion constructs, Ct-KDC1-ΔK_{HA} and Ct-KDC1-cNBD, were tested in the yeast two-hybrid system
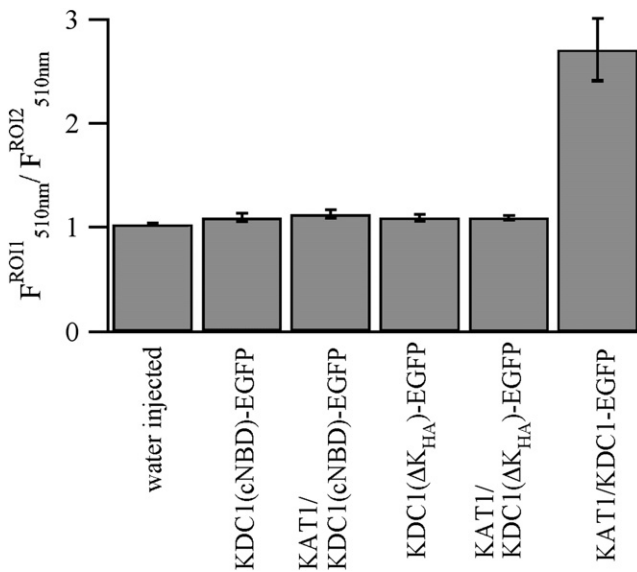
FIGURE 4 Truncated KDC1 constructs, alone or coinjected with KAT1, are not targeted to the plasma membrane. Relative fluorescence at 510 nm measured at the external layer of the oocyte (ROI1), normalized to the fluorescence measured outside the oocyte (ROI2) for the different constructs KDC1(cNBD)-EGFP and KDC1(ΔK_{HA})-EGFP injected alone or coinjected with KAT1. Data are shown as mean $\pm$ SE from >9 ROI.

together with Ct-KAT1, no evidences for physical protein-protein interactions were obtained anymore (Fig. 3 B). Thus, it appears that the K_{HA}-domain of KDC1 is responsible for the interaction with the KAT1 C-terminus.

Fluorescence points out that without K_{HA} domain KDC1-EGFP is not targeted to the oocyte membrane

Looking for a confirmation of the loss of interaction observed in the yeast two-hybrid system when the K_{HA} segment was deleted, we investigated the properties of truncated KDC1 by means of fluorescence measurements. To this purpose, we generated the two deletions in the cDNA coding for the full-length KDC1, fused them at the 3'-end with the coding region of EGFP, and expressed these constructs in *Xenopus* oocytes alone or in coexpression with the unlabeled KAT1. Similarly to the full-length KDC1-EGFP expressed alone (Fig. 1, E and G), no GFP signal could be detected at the membrane of oocytes expressing KDC1(ΔK_{HA})-EGFP and KDC1(cNBD)-EGFP, respectively, neither when they were injected alone nor together with KAT1 (Fig. 4). Moreover the injection of the cytosolic marker Fura Red in

oocytes expressing KAT1/KDC1(ΔK_{HA})-EGFP and KAT1/KDC1(cNBD)-EGFP did not show any variation of the fluorescence results. The distances between the two peaks identifying the two fluorophores, d(EGFP-Fura Red), are shown in Table 1. Thus, without the amino acids downstream of the cNBD or the K_{HA} domain, KDC1 is not targeted to the plasma membrane of oocytes even when it is coinjected with KAT1.

The K_{HA} domain of KDC1 is important but not essential for the KDC1 heteromerization with KAT1

The functional consequences of the loss of interaction (Fig. 3 B) and the loss of channel targeting (Fig. 4) were assayed by electrophysiological experiments. Control experiments demonstrated that neither the injection of KDC1 in *Xenopus* oocytes nor that of KDC1(cNBD) or KDC1(ΔK_{HA}) resulted in currents different from the baseline (oocyte injected with H_2O) (Fig. 5 A).

Then, the coexpression with KAT1 was tested. KAT1 was expressed alone or coexpressed with KDC1, KDC1(ΔK_{HA}), and KDC1(cNBD), respectively. In all cases inward-rectifying K^+-selective currents were measured (Fig. 5 B). The different susceptibility of KAT1 and KDC1 toward Zn^{2+} (KAT1 is blocked whereas KAT1/KDC1 currents are stimulated by Zn^{2+}) was used as a marker to demonstrate the formation of heteromeric KAT1/KDC1 channels (15,18,19). When 1 mM Zn^{2+} was added to the bathing medium, the current increased in the case of the KAT1/KDC1 pair, whereas it decreased, to a different extent, in the other two pairs (Fig. 5 C). Indeed, the KAT1/KDC1(cNBD) pair displayed a zinc inhibition of the current very similar to that observed for KAT1 alone (Fig. 5 C, left panel), whereas the decrease of the current of the KAT1/KDC1(ΔK_{HA}) pair was less pronounced and statistically different from that observed on KAT1. Therefore, quantitative electrophysiological data suggest that KDC1 lacking the K_{HA} domain actually still marginally interacts with KAT1.

To provide further information on a possible effect of EGFP (attached at the C-terminal domain) on heteromerization as well as functionality of the channel, electrophysiological experiments were also done on the fluorescent constructs KDC1(ΔK_{HA})-EGFP and KDC1(cNBD)-EGFP coexpressed with KAT1 (Fig. 6). Also in these cases zinc was added to the external solution to test the metal susceptibility of the channels. At −160 mV no differences were observed between KAT1 and the two coexpressed channels; this suggest that when GFP was present no heteromeric KAT1/

TABLE 1 Values ($\pm$ combined SE) of the distances between the peaks of fluorescence intensity of the two fluorophores (EGFP and Fura Red) for the wild-type and the truncated channels ($N \geq 8$)

	KAT1	KAT1/KDC1	KDC1	KAT1/ KDC1(cNBD)	KAT1/KDC1(ΔK_{HA})	KDC2/KDC1
d(EGFP-Fura Red)	2.6 $\pm$ 0.3 (+)	2.5 $\pm$ 0.3 (+)	−0.5 $\pm$ 0.3 (−)	−0.8 $\pm$ 0.4 (−)	−0.6 $\pm$ 0.4 (−)	2.1 $\pm$ 0.3 (+)

The $\pm$ labels indicate when EGFP is external (+) or internal (−) with respect to Fura Red.
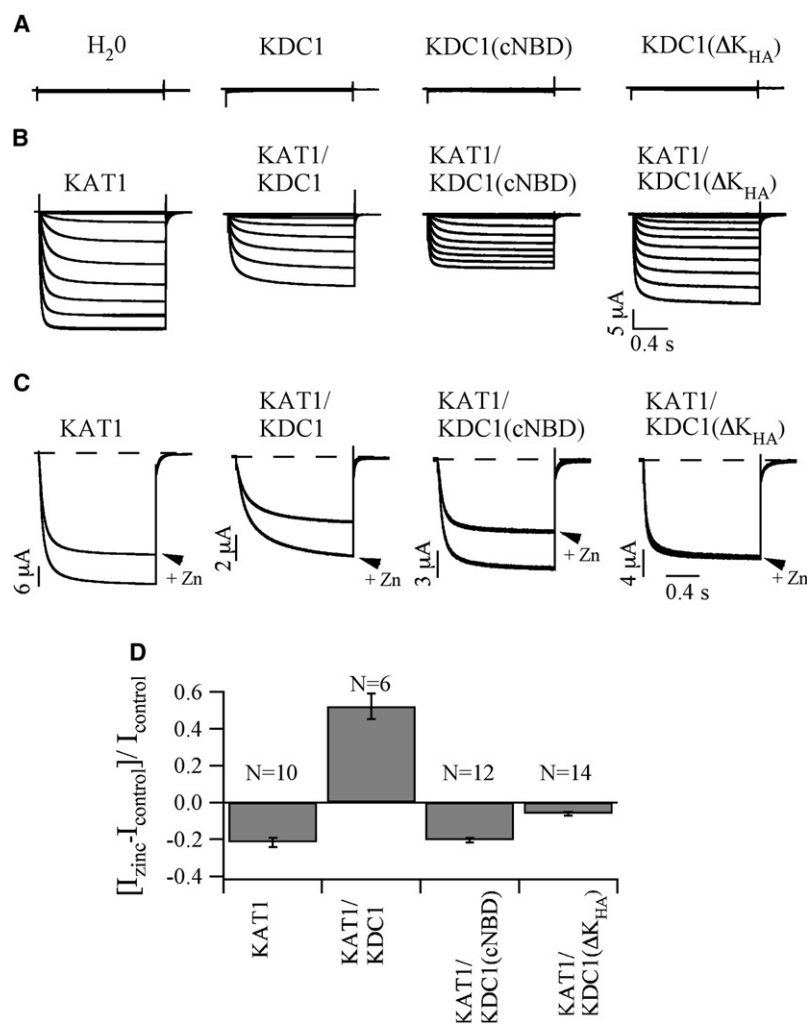
FIGURE 5 Electrophysiological analysis of the homomeric and heteromerized truncated constructs. Current traces recorded in oocytes injected with the full-length construct KDC1 and the truncated constructs KDC1(cNBD) and KDC1(ΔK_{HA}) (*A*) and the same constructs coinjected with KAT1(*B*). (*C*) Comparison $\pm$ Zn^{2+} at -160 mV for KAT1 and KAT1 coinjected with KDC1 or with the truncated KDC1 constructs. (*D*) Change of the current induced by 1 mM Zn^{2+} at -160 mV (I_{zinc}-$I_{control}$)/$I_{control}$ for the same constructs of panel *C*. Data are shown as mean $\pm$ SE. The values obtained for the KAT1/KDC1(ΔK_{HA}) pair were significantly larger than the values obtained for KAT1 (Student's *t*-test, $p < 0.0001$), whereas the values obtained for the KAT1/KDC1(cNBD) pair were not ($p = 0.77$).

KDC1(ΔK_{HA})-EGFP channels were formed. Presumably, the presence of the large GFP protein, attached at the C-terminus, definitely compromises the already critical interaction between KAT1 and the ΔK_{HA} truncated form of KDC1. Moreover, also when the EGFP was attached at the N-terminus, heteromerization capability between KAT1 and KDC1 was decreased (Fig. 6 *B*). Indeed, the enhancement of the current induced by zinc was comparable in KAT1/KDC1-EGFP and KAT1/EGFP-KDC1, but lower compared to that observed in the heteromeric wild type KAT1-KDC1.

Detailed analysis pointed out that the open probability characteristics (Fig. 7 *A*) and the kinetics (Fig. 7 *B*) (illustrated by the slower component of the activation time constant, τy) of the homomeric KAT1 channel were almost identical to those of the KAT1/KDC1(cNBD) combination but different from those of KAT1/KDC1(ΔK_{HA}). These lines of evidences confirm that some heteromeric KAT1/KDC1(ΔK_{HA}) complexes are still present. Instead, when the EGFP protein was attached to the construct, heteromeric channel formation was compromised as demonstrated by the comparison of Boltzmann curves in Fig. 7 *A*. This confirms that EGFP attached to wild-type KDC1 has a negative effect on heteromerization, as suggested

from the shift of the open probability of KAT1/KDC1-EGFP to less negative voltages (i.e., closer to homomeric KAT1 characteristics, Fig. 7 *A*) and in agreement with the results obtained previously from the inhibition of ionic current by zinc (Fig. 6 *B*). Moreover, the open probability analysis provides further support to the equivalence of EGFP tagging at the C- or N-terminus of KDC1. Interestingly, the formation of heteromeric complexes influences the apparent gating charge derived from the Boltzmann distribution in Fig. 7 *A* ($z < 1.3$ for the heteromeric and $z > 1.6$ for the homomeric channels).

Finally, we verified the physiological significance of the results obtained on the KDC1/KAT1 model system by replacing the *Arabidopsis* KAT1 by KDC2, a KAT1-homolog from carrot (23). Like KAT1, KDC2 expresses functional channels when injected alone in *Xenopus* oocytes (23). We could verify by confocal fluorescence measurements and electrophysiological analyses that, similarly to KAT1 (Fig. 2), KDC2 forms heteromeric channels with KDC1 (Fig. 8 *B*) targeting KDC1 to the oocyte membrane (Fig. 8 *A* and Table 1). Expression of KDC2 with the truncated KDC1 constructs demonstrated that also the heteromerization of these two subunits was abolished by the cNBD deletion (Fig. 8 *B*). On the contrary, deletion of
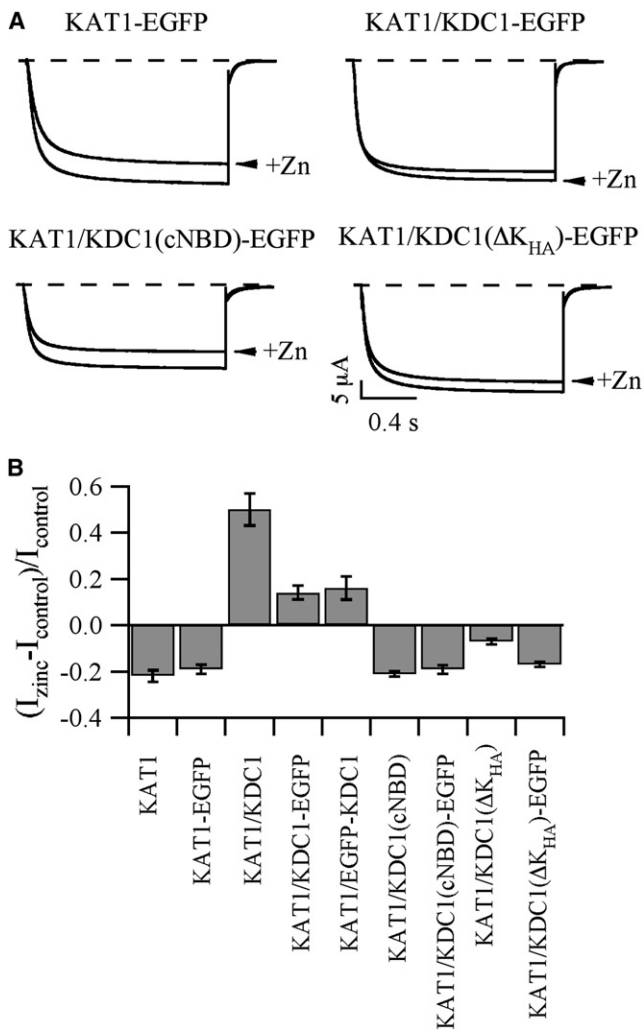
FIGURE 6 Effect of zinc on the heteromeric EGFP constructs. (*A*) Comparison ± 1 mM Zn^{2+} at -160 mV for KAT1-EGFP and KAT1 coinjected with KDC1-EGFP or the truncated KDC1-EGFP constructs. (*B*) Change of the current induced by 1 mM Zn^{2+} at -160 mV (I_{zinc}-$I_{control}$)/$I_{control}$ for all the studied constructs. Data are shown as mean $\pm$ SE ($N \geq 7$).

the K_{HA} domain determined a decrease of the macroscopic current but did not abolish the interaction of KDC2 and KDC1-ΔK_{HA} as demonstrated by the KDC1-specific zinc phenotype.

DISCUSSION

We addressed the problems of localization and contribution to heteromerization by different segments of plant *Shaker*-like inward-rectifying potassium channels by using different approaches: a), confocal microscopy was adopted to verify if the channels are localized or not in the membrane of oocytes injected with different cocktails of subunit-encoding RNAs, b), the yeast two-hybrid system provided information on the role played by different parts of the C-terminus in the interactions of diverse subunits, c), electrophysiology experi-
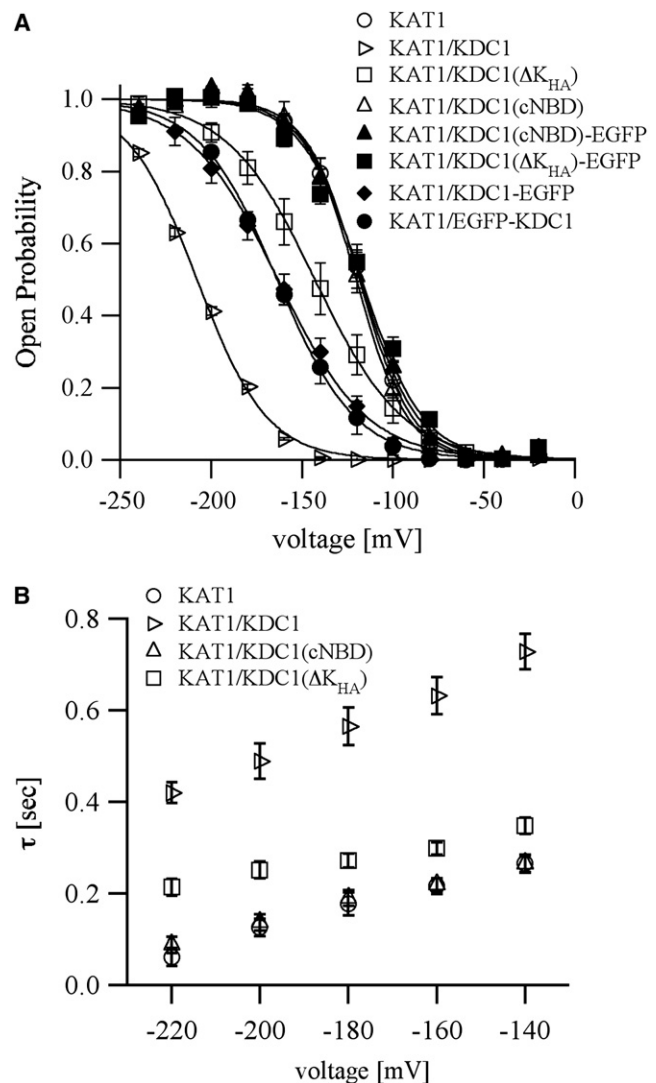

FIGURE 7 Open probability and kinetics of channels obtained from the coexpression of KAT1 and different KDC1 constructs, either tagged or untagged with GFP. (*A*) Open probability characteristics of the homomeric KAT1 channel, the heteromeric KAT1/KDC1 channel, and channels obtained coexpressing KAT1 with truncated KDC1 with and without EGFP. Data were obtained from steady state currents like those shown in Fig. 5. Continuous curves are the best fit of the mean open probability ($\pm$ SE) obtained from at least seven experiments for each construct yielding the following values: KAT1($V_{1/2} = -119$ mV, $z = 1.7$); KAT1/KDC1($V_{1/2} = -208$ mV, $z = 1.3$); KAT1/KDC1-EGFP($V_{1/2} = -163$ mV, $z = 1.0$); KAT1/EGFP-KDC1($V_{1/2} = -164$ mV, $z = 1.1$); KAT1/KDC1(cNBD) ($V_{1/2} = -120$ mV, $z = 1.7$); KAT1/KDC1(ΔK_{HA}) ($V_{1/2} = -143$ mV, $z = 1.0$); KAT1/KDC1(cNBD)-EGFP($V_{1/2} = -118$ mV, $z = 1.6$); KAT1/KDC1(ΔK_{HA})-EGFP ($V_{1/2} = -117$ mV, $z = 1.3$). (*B*) Activation current traces of the investigated channels were fitted with two exponentials and the activation time constant of the slower exponential, τ_2, was plotted versus the applied potential. It can be observed that the activation time constant, τ_2, for the construct KAT1/KDC1(ΔK_{HA}) significantly differs from that observed for KAT1 (Student's *t*-test, ranging from $p < 0.002$ to $p < 0.0001$). Data are mean $\pm$ SE of at least seven experiments.

ments performed on *Xenopus* oocytes provided information about the functional properties of diverse homomeric and heteromeric aggregates.
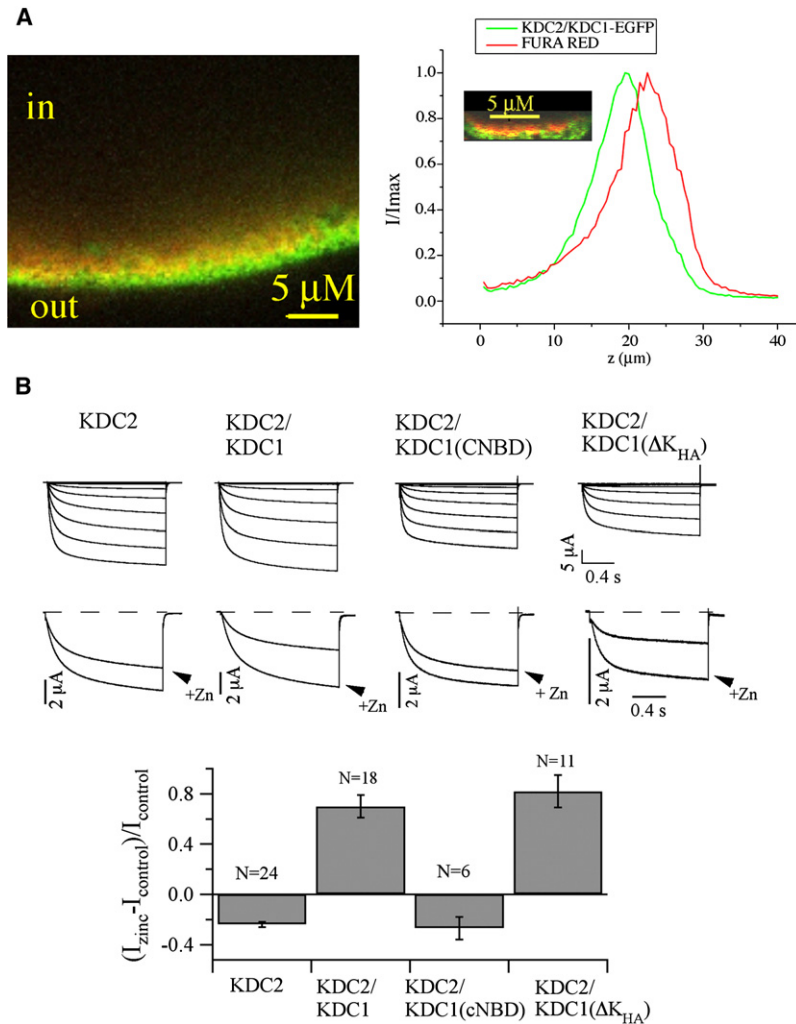
FIGURE 8 Heteromerization between KDC1 and KDC2 channel subunits. (*A*) KDC1 is targeted to the membrane when it is coexpressed with KDC2. Confocal laser-scanning microscopical analyses on oocytes expressing KDC2/KDC1-EGFP microinjected with Fura Red. The left column shows the fluorescence collected from an *x-y* plane of the oocyte. This panel shows a green layer (belonging to GFP signal) external to the red one (belonging to Fura Red signal); the yellow layer is due to the colocalization of the two fluorophores. The right column shows the results obtained by a spectral unmixing analysis, applied on every oocyte injected. Traces show normalized fluorescence intensity for a particular ROI of the two fluorophores as a function of the distance *z* (0 coincides with the slide plane and 40 μm with the most internal plane of the oocyte reached). The inset shows a magnification of the distance between the two fluorophores. The mean distance measured between the two peaks, d(EGFP-Fura Red), is 2.1 $\pm$ 0.3 μm. Data are mean values $\pm$ SE from more than 20 ROI on seven independent oocytes. (*B*) Upper panel: current traces recorded in oocytes injected with KDC2 and KDC2 coinjected with KDC1 and the truncated constructs KDC1(cNBD) and KDC1(ΔK_{HA}). Middle panel: comparison $\pm$ Zn^{2+} at -160 mV for the same constructs. Lower panel: mean values ($\pm$ SE) of the change of the current induced by 1 mM Zn^{2+} at -160 mV ($I_{zinc}-I_{control})/I_{control}$ for the different constructs.

To this purpose we selected the silent potassium channel KDC1, which, in *Xenopus* oocytes, does not form homomeric functional channels by itself; instead, KDC1 subunits participate, with other inward rectifying potassium channel subunits, in the formation of functional heteromeric channels. The presence of KDC1 subunits in heteromeric channels can be conveniently monitored by the channel response to zinc added to the bath solution. Indeed, unlike other voltage-dependent plant potassium channels, this type of heteromeric channels displays currents that are potentiated by zinc.

Localization

KDC1-EGFP displayed in oocytes only in 20% of the experiments EGFP fluorescence at the oocyte external surface. This could be interpreted as a limited expression efficiency of KDC1 in oocytes. However, electrophysiological experiments performed on these fluorescent oocytes did not reveal any potassium current.

To clarify this point a more accurate localization and analysis of channel bound EGFP was necessary. To this purpose,

we injected Fura Red as a cytosolic marker in oocytes expressing the EGFP-fusion construct. The spectral unmixing technique helped to define more precisely the relative position of membrane and cytosol (35). Indeed, unlike KAT1-EGFP and coexpressed KAT1/KDC1-EGFP, KDC1-EGFP colocalized with Fura Red; thus suggesting that actually, KDC1 alone was never targeted to the plasma membrane. This fluorescence signal could derive from the endoplasmatic reticulum being very close to the inner surface of the oocyte (35–37). Endoplasmic reticulum retention has been observed for several other regulatory potassium channel α-subunits (20,21).

Differently from many heterologously expressed membrane proteins that are typically targeted to the animal hemisphere (35,38), KAT1-EGFP and KAT1/KDC1-EGFP were uniformly targeted to both animal and vegetal hemispheres (data not shown).

No difference was observed in electrophysiogical control experiments when EGFP was attached to the N- or C-terminus (i.e., EGFP-channel or channel-EGFP form) of the channel (Figs. 6 *B* and 7 *A*). Vice versa, when we looked at the

fluorescent constructs by confocal microscopy, a diffuse and unclustered fluorescence signal was occasionally observed in the case of the EGFP-channel constructs. Therefore, to rule out the possibility to work with free soluble EGFP, in our experiments, we used the C-terminal fusions (channel-EGFP forms).

Contribution of segments to heteromerization

Many previous studies have shown that the C-terminus of the channel is involved in the functional expression of plant potassium channels (11,32,34). It has been demonstrated that the deletion of the region before the cNBD of the KAT1 channel inhibits the expression of this channel, whereas other deletions on C- or N-termini change the voltage dependence but not the expression (33). Recently the diacidic motif DAE, upstream the cNBD of KAT1, was demonstrated to be crucial for the transfer of functional channels from the endoplasmic reticulum to plasma membrane (39). However, point mutation in the KDC1 amino-acid sequence (K396D-A-E) failed to transform KDC1 from a silent to a functional subunit (data not shown). Moreover, also a KDC1 chimera where the C-terminus of KDC1 was substituted with the C-terminus of KAT1 did not express functional channels in *Xenopus* oocytes (data not shown).

To date, some results provided information on parts of the C-terminus that favor the interaction between different subunits of *Shaker*-like channels. Usually, the region that is involved in the interaction between different α-subunits depends on the type of channel under investigation. Indeed, only some inward rectifying subunits present an ankyrin domain in the C-terminus, which cooperates to the interaction with other homologous proteins (32). The C-terminus characteristics seem also to be responsible for the prevention of heteromeric complexes between inward and outward rectifying channels (11).

To investigate which segments of the protein are involved in the heteromerization of KDC1, we deleted the last part of the protein downstream the cNBD (134 amino acids) or the distal part of the C-terminus K_{HA} (51 amino acids). By the two-hybrid system, no interaction was observed between both deleted KDC1 C-terminus constructs and the C-terminus of KAT1. Similar consistent results were also obtained from fluorescence experiments. The absence of EGFP clusters at the external layer of the oocytes indicated that deletion of the K_{HA} domain prevented formation of heteromeric complexes. Instead, although ionic currents of oocytes injected with KAT1/KDC1(cNBD), challenged by the addition of Zn^{2+} and by its biophysical characteristics, did not show any appreciable presence of KDC1(cNBD) in the functional channels, a slight heteromerization capability was observed in electrophysiological experiments performed on oocytes injected with KAT1 and the deleted KDC1(ΔK_{HA}) construct. Indeed, the inhibition of the current induced by zinc was less pronounced than in the homomeric KAT1 channel although

we never observed any increase of the current as we did in the heteromeric KAT1/KDC1 channel (see Fig. 6 and (18)). Last doubts on the formation of heteromeric KAT1/KDC1(ΔK_{HA}) channels were ruled out by analyzing the voltage-dependence of the channel open probability. The characteristics of KAT1/KDC1(ΔK_{HA}) were different from those of heteromeric KAT1/KDC1 channels but also different from those of homomeric KAT1 channels (Fig. 7).

The results obtained from coexpressing KDC1 with KAT1 were in good qualitative agreement with those observed for the pair KDC1 and KDC2. Deletion of the region downstream of the cNBD completely abolished the capability of KDC1 to form heteromers with KDC2 and deletion of the K_{HA} domain reduced heteromeric channel formation. The smaller currents $(I_{-160}(KDC2/KDC1(\Delta K_{HA}))= -0.9 \pm 0.2 \mu A$ with respect to $I_{-160}(KDC2/KDC1)= -5.4 \pm 1.2 \mu A$ and to $I_{-160}(KDC2)= -10.7 \pm 2.6 \mu A$ and Fig. 8 B) together with the large zinc potentiation of the KDC2/KDC1(ΔK_{HA}) subunits suggest that a smaller number of functional channels are expressed and that the majority of them are heterometers. Interestingly, identities between KDC2 and KAT1 subunits are higher in the cytosolic N-terminus (67%) and the channel transmembrane core (83%), but slightly lower (59%) in the first part of the cytosolic C-terminus (compare Fig. 3 A, iv) and much lower (35%) in the second part of the C-terminus (compare Fig. 3 A, v), which was identified in our study to be essential for the KAT1/KDC1 interaction.

All together, the experiments performed on the truncated forms of KDC1 suggest that the deletion of the last 134 amino acids is crucial for the heteromerization capability of KDC1 with KAT1 and KDC2, whereas the deletion of the last 51 amino acids is not sufficient to fully prevent heteromerization. This result is slightly different from previous findings on the potato guard cell channels KST1 and SKT1 (10,34). Although also here the deletion of the last 141 amino acids in SKT1 (including the K_{HA} and a so-called K_T domain) resulted in a loss of the ability of this subunit to heteromerize with KST1, the deletion of only the K_{HA}-domain (last 75 amino acids) had no negative effect on the heteromerization process (10).

Interestingly, the discrepancy between the results obtained by electrophysiology and fluorescence studies might depend on the presence of EGFP. We wonder whether truncated constructs with or without EGFP may display a different subunit assembly capability between KDC1 and KAT1 probably owing to the steric hindrance of the large EGFP molecule attached to the carboxiterminus. Electrophysiology experiments confirm that no evident heteromerization occurs when the green fluorescent protein is attached to KDC1(ΔK_{HA}). Moreover, EGFP affects heteromerization also when attached to the protein N-terminus that typically is not involved in subunit assembly. Precisely, control experiments on KAT1/KDC1 channels and on KAT1/KDC1(EGFP), where EGFP was attached either to the N- or to the C-terminus, demonstrated a significant difference in the zinc effects (Fig. 6 B)

and different open probabilities of KAT1/KDC1-EGFP and KAT1/EGFP-KDC1 with respect to wild-type KAT1/KDC1 (Fig. 7 A). Indeed, all these evidences point to an interference of EGFP with the assembly process.

CONCLUSION

The presented data indicate that KDC1 is an auxiliary subunit incapable to form functional K^+ channels on its own. The protein is not targeted to the membrane. Upon coexpression with KAT1 or with the physiological partner KDC2, the two subunits form heteromeric channels, which are then targeted to the membrane. Heteromerization depends on regions within the last 134 amino acids of the KDC1 protein. Deletion of the K_{HA}-domain (last 51 amino acids) weakens but does not fully suppress the heteromerization process. Protein fusions with GFP also had a negative influence on the heteromerization capability. Our data indicate that results on ion channels obtained with channel-GFP fusion constructs may not necessarily reflect the behavior of the untagged channel.

REFERENCES

1. Schroeder, J. I., and R. Hedrich. 1989. Involvement of ion channels and active transport in osmoregulation and signaling of higher plant cells. *Trends Biochem. Sci.* 14:187–192.

2. Véry, A. A., and H. Sentenac. 2003. Molecular mechanisms and regulation of K^+ transport in higher plants. *Annu. Rev. Plant Biol.* 54:575–603.

3. Amtmann, A., P. Armengaud, and V. Volkov. 2004. Potassium nutrition and salt stress. *In* Membrane Transport in Plants. M. R. Blatt, editor. Blackwell, Oxford, pp. 316–348.

4. Dreyer, I., E. Michard, B. Lacombe, and J. B. Thibaud. 2001. A plant *Shaker*-like K^+ channel switches between two distinct gating modes resulting in either inward-rectifying or "leak" current. *FEBS Lett.* 505:233–239.

5. Michard, E., I. Dreyer, B. Lacombe, H. Sentenac, and J. B. Thibaud. 2005. Inward rectification of the AKT2 channel abolished by voltage-dependent phosphorylation. *Plant J.* 44:783–797.

6. Michard, E., B. Lacombe, F. Porée, B. Mueller-Roeber, H. Sentenac, et al. 2005. A unique voltage-sensor sensitizes the potassium channel AKT2 to phosphoregulation. *J. Gen. Physiol.* 126:605–617.

7. Yu, L., D. Becker, H. Levi, M. Moshelion, R. Hedrich, et al. 2006. Phosphorylation of SPICK2, an AKT2 channel homologue from Samanea motor cells. *J. Exp. Bot.* 57:3583–3594.

8. Dreyer, I., S. Antunes, T. Hoshi, B. Müller-Röber, K. Palme, et al. 1997. Plant K^+ channel α-subunits assemble indiscriminately. *Biophys. J.* 72:2143–2150.

9. Pilot, G., B. Lacombe, F. Gaymard, I. Cherel, J. Boucherez, et al. 2001. Guard cell inward K^+ channel activity in arabidopsis involves expression of the twin channel subunits KAT1 and KAT2. *J. Biol. Chem.* 276:3215–3221.

10. Zimmermann, S., S. Hartje, T. Ehrhardt, G. Plesch, and B. Müller-Röber. 2001. The K^+ channel SKT1 is co-expressed with KST1 in potato guard cells both channels can co-assemble via their conserved KT domains. *Plant J.* 28:517–527.

11. Dreyer, I., F. Poree, A. Schneider, J. Mittelstadt, A. Bertl, et al. 2004. Assembly of plant *Shaker*-like K_{out} channels requires two distinct sites of the channel alpha-subunit. *Biophys. J.* 87:858–872.

12. Baizabal-Aguirre, V. M., S. Clemens, N. Uozumi, and J. I. Schroeder. 1999. Suppression of inward-rectifying K^+ channels KAT1 and AKT2 by dominant negative point mutations in the KAT1 a-subunit. *J. Membr. Biol.* 167:119–125.

13. Ache, P., D. Becker, R. Deeken, I Dreyer, H. Weber, et al. 2001. VFK1, a Vicia faba K^+ channel involved in phloem unloading. *Plant J.* 27:571–580.

14. Xicluna, J., B. Lacombe, I. Dreyer, C. Alcon, L. Jeanguenin, et al. 2007. Increased functional diversity of plant K+ channels by preferential heteromerization of the *Shaker*-like subunits AKT2 and KAT2. *J. Biol. Chem.* 282:486–494.

15. Paganetto, A., M. Bregante, P. Downey, F. Lo Schiavo, S. Hoth, et al. 2001. A novel K^+ channel expressed in carrot roots with a low susceptibility toward metal ions. *J. Bioenerg. Biomembr.* 33:63–71.

16. Reintanz, B., A. Szyroki, N. Ivashikina, P. Ache, M. Godde, et al. 2002. AtKC1, a silent Arabidopsis potassium channel alfa-subunit modulates root hair K^+ influx. *Proc. Natl. Acad. Sci. USA.* 99:4079–4084.

17. Formentin, E., S. Varotto, A. Costa, P. Downey, M. Bregante, et al. 2004. DKT1, a novel K^+ channel from carrot, forms functional heteromeric channels with KDC1. *FEBS Lett.* 573:61–67.

18. Picco, C., M. Bregante, A. Naso, P. Gavazzo, A. Costa, E. Formentin, P. Downey, F. Lo Schiavo, and F. Gambale. 2004. Histidines are responsible for zinc potentiation of the current in KDC1 carrot channels. *Biophys. J.* 86:224–234.

19. Naso, A., R. Montisci, F. Gambale, and C. Picco. 2006. Stoichiometry studies reveal functional properties of KDC1 in plant *Shaker* potassium channels. *Biophys. J.* 91:1–11.

20. Bregante, M., Y. Yang, E. Formentin, A. Carpaneto, J. I. Schroeder, et al. 2008. KDC1, a carrot *Shaker*-like potassium channel, reveals its role as a silent regulatory subunit when expressed in plant cells. *Plant Mol. Biol.* 66:61–72.

21. Duby, G., E. Hosy, C. Fizames, C. Alcon, A. Costa, et al. 2008. AtKC1, a conditionally targeted *Shaker*-type subunit, regulates the activity of plant K+ channels. *Plant J.* 53:115–123.

22. Downey, P., I. Szabò, N. Ivashikina, A. Negro, F. Guzzo, et al. 2000. Kdc1 a novel carrot root hair K^+ channel: cloning, characterisation and expression in mammalian cells. *J. Biol. Chem.* 275:39420–39426.

23. Formentin, E., A. Naso, S. Varotto, C. Picco, F. Gambale, et al. 2006. KDC2, a functional homomeric potassium channel expressed during carrot embryogenesis. *FEBS Lett.* 580:5009–5015.

24. Ausubel, F. M., R. Brent, R. E. Kingston, D. D. Moore, J. G. Seidman, et al. 1997. Current protocols in molecular biology. John Wiley & Sons, New York.

25. Tsurui, H., H. Nishimura, S. Hattori, S. Hirose, K. Okumura, et al. 2000. Seven-color fluorescence imaging of tissue samples based on Fourier spectroscopy and singular value decomposition. *J. Histochem. Cytochem.* 48:653–662.

26. Zimmermann, T., J. Rietdorf, and R. Pepperkok. 2003. Spectral imaging and its applications in live cell microscopy. *FEBS Lett.* 546:87–92.

27. Huth, U., A. Wieschollek, Y. Garini, R. Schubert, and R. Peschka-Suss. 2004. Fourier transformed spectral bio-imaging for studying the intracellular fate of liposomes. *Cytometry A.* 57:10–21.

28. Taraldsen, G. 2006. Instrument resolution and measurement accuracy. *Metrologia.* 43:539–544.

29. van der Ven, P. F., S. Wiesner, P. Salmikangas, D. Auerbach, M. Himmel, et al. 2000. Indications for a novel muscular dystrophy pathway. gamma-filamin, the muscle-specific filamin isoform, interacts with myotilin. *J. Cell Biol.* 151:235–248.

30. Zampighi, G. A., D. D. Loo, M. Kreman, S. Eskandari, and E. M. Wright. 1999. Functional and morphological correlates of connexin50 expressed in Xenopus laevis oocytes. *J. Gen. Physiol.* 113:507–524.

31. Sutter, J. U., P. Campanoni, M. Tyrrell, and M. R. Blatt. 2006. Selective mobility and sensitivity to SNAREs is exhibited by the Arabidopsis KAT1 K+ channel at the plasma membrane. *Plant Cell.* 18:935–954.

32. Daram, P., S. Urbach, F. Gaymard, H. Sentenac, and I. Cherel. 1997. Tetramerization of the AKT1 plant potassium channel involves its C-terminal cytoplasmic domain. *EMBO J.* 16:3455–3463.

33. Marten, I., and T. Hoshi. 1997. Voltage-dependent gating characteristics of the K$^+$ channel KAT1 depend on the N and C termini. *Proc. Natl. Acad. Sci. USA.* 94:3448–3453.

34. Ehrhardt, T., S. Zimmermann, and B. Muller-Rober. 1997. Association of plant K$^+_{in}$ channels is mediated by conserved C-termini and does not affect subunit assembly. *FEBS Lett.* 409:166–170.

35. Subramanian, V. S., J. S. Marchant, I. Parker, and H. M. Said. 2001. Intracellular trafficking/membrane targeting of human reduced folate carrier expressed in Xenopus oocytes. *Am. J. Physiol. Gastrointest. Liver Physiol.* 281:G1477–G1486.

36. Singer-Lahat, D., N. Dascal, L. Mittelman, S. Peleg, and I. Lotan. 2000. Imaging plasma membrane proteins in large membrane patches of Xenopus oocytes. *Pflugers Arch.* 440:627–633.

37. Ottolia, M., K. D. Philipson, and S. John. 2007. Xenopus oocyte plasma membrane sheets for FRET analysis. *Am. J. Physiol. Cell Physiol.* 292:C1519–C1522.

38. Balduzzi, R., A. Cupello, A. Diaspro, P. Ramoino, and M. Robello. 2001. Confocal microscopic study of GABA(A) receptors in Xenopus oocytes after rat brain mRNA injection: modulation by tyrosine kinase activity. *Biochim. Biophys. Acta.* 1539:93–100.

39. Mikosch, M., A. C. Hurst, B. Hertel, and U. Homann. 2006. Diacidic motif is required for efficient transport of the K+ channel KAT1 to the plasma membrane. *Plant Physiol.* 142:923–930.